Available online at www.sciencedirect.com
ScienceDirect
Journal of Food Engineering 88 (2008) 65–74
JOURNAL OF FOOD ENGINEERING
www.elsevier.com/locate/jfoodeng

Effect of processing parameters on foam formation using a continuous system with a mechanical whipper

Linda Indrawati [a], Zebin Wang [a], Ganesan Narsimhan [a,*], Juan Gonzalez [b]

[a] Department of Agricultural and Biological Engineering, Purdue University, West Lafayette, IN 47907, USA
[b] Nestlé R&D Center, Inc., New Milford, CT, USA

Received 31 July 2007; received in revised form 15 January 2008; accepted 19 January 2008
Available online 26 January 2008

Abstract

A continuous system with a mechanical whipper was designed to make protein stabilized foams. Three different impellers (four-blade, six-blade-straight and six-blade-curve disc) were employed to make foams stabilized by sodium caseinate and whey protein. The inlet liquid flow rate of protein solution was varied in the range of 5–15 mL/s, the whipper speed in the range of 5000–15,000 rpm and temperature ranged from 21 to 80 °C. The effects of whipper speed, flow rate, type of protein, temperature and whipper geometry on foamability, foam stability, power input, apparent viscosity index and bubble size distribution of foams were investigated. Higher foaming capacity was observed at higher whipper speeds, lower liquid flow rates, and in the case of sodium caseinate stabilized foams. The power input was found to be highest for the lowest liquid flow rate. A six-blade curved impeller rotating along and opposite to the direction of the curvature of vanes produced the most foam and smallest bubble size, respectively. Higher temperatures resulted in better foam stability for foams formed with whey protein whereas it had detrimental effect on foam stability with sodium caseinate.

Keywords: Whipping; Protein stabilized foam; Bubble size; Temperature; Foam formation; Sodium caseinate; Whey protein; Mechanical whipper

1. Introduction

Foam is a high volume fraction of gas dispersed in liquid and has a variety of applications including beer, bread, whipped cream, ice cream, meringue and marshmallow. Foams are thermodynamically unstable and will break down eventually. Therefore, a surface active agent such as protein is used to provide kinetic stability. Protein reduces the surface tension which facilitates foam formation and stabilizes the foam system by modifying the interparticle forces between foam bubbles and by enhancing the interfacial rheology. The effectiveness of protein as a food emulsifier is related to its rate of adsorption at the interface. It has been shown (Graham and Phillips, 1979; Cho et al., 1996, 1997) that protein adsorption is influenced by molecular properties, such as size, shape, surface hydrophobicity, conformation, and charge as well as by conditions in the bulk solution, such as bulk concentration, pH and ionic strength. In addition to decreasing the interfacial tension, proteins provide rheological properties, such as a high shear viscosity and dilatational modulus, which help stabilize the foam (Mita et al., 1977; Graham and Phillips, 1979; Damodaran, 1996).

Foaming properties are often characterized by foaming capacity and foam stability. Foaming capacity or foamability (Prins, 1988) is defined as the capacity of the continuous phase to entrap air or gas, and foam stability as the ability to retain the gas for a certain period of time. The foaming properties of protein foams depend on many intrinsic factors (size, structure of protein, hydrophobicity, surface potential, charge, etc.); and environmental and processing factors (protein concentration, pH, temperature, addition of other ingredients, etc.). Earlier studies have found that increasing protein concentration results in increasing rate of adsorption of protein at the air–water interface, leading

* Corresponding author. Tel.: +1 765 494 1199; fax: +1 765 496 1115.
E-mail address: narsimha@purdue.edu (G. Narsimhan).

0260-8774/$ - see front matter © 2008 Elsevier Ltd. All rights reserved.
doi:10.1016/j.jfoodeng.2008.01.015

to a reduction in surface tension, and hence an increase in the foaming capacity (Patino et al., 1995; Cho et al., 1996, 1997; Cornec et al., 2001; Wang and Narsimhan, 2004). The foaming capacity is also markedly affected by molecular size and structure of protein. Disordered, small and flexible proteins reduce the surface tension earlier and faster than ordered, rigid and larger proteins (Graham and Phillips, 1979; Dickinson and Stainsby, 1982; Martin et al., 2002), therefore they have higher foaming capacity. Several studies have shown that the foamability of many proteins is significantly improved near their isoelectric point (Buckingham, 1970; Mita et al., 1978; Yu and Damodaran, 1991; Narsimhan and Uraizee, 1992). Other studies suggest that heat denaturation of whey protein improves foaming properties (deVilbiss et al., 1974; Haggett, 1976; de Wit et al., 1986). This increase in foaming capacity is due to the increase in surface hydrophobicity upon denaturation (Mitchell, 1986), which decreases the energy barrier for adsorption, allowing for a faster rate of adsorption at the air–water interface.

Globular protein results in higher foam stability due to its ability to form cohesive, elastic and viscous film (Phillips, 1981). The formation of multilayer of globular proteins increases with protein concentration (Graham and Phillips, 1976, 1980) and provides stability to the foams (Damodaran, 1996). The increase in bulk viscosity due to the addition of xanthan gum has been shown to improve the drainage stability (Carp et al., 1997). Foam stability is mostly significantly improved in the region close to the isoelectric point of proteins (pI), where electrostatic repulsion is minimum (Yu and Damodaran, 1991) and thicker protein films with improved rheological properties are formed. The improved rheological properties retard the liquid drainage which provides for better foam stability (Mita et al., 1977; Graham and Phillips, 1980). It has been observed (Patino et al., 1995) that casein stabilized foams are more stable at room temperature than when the temperature is increased. At high temperatures, the interaction between the proteins is greater when the protein is denatured, which promotes coagulation and precipitation (Oortwijn and Walstra, 1979) and lowers the surface activity. Furthermore, the increase in temperature reduces the viscosity of continuous phase and causes instability in the foam (Mita et al., 1977; Halling, 1981). However, some studies have shown that heat denaturation of whey protein not only improves the foaming capacity, but also foam stability (deVilbiss et al., 1974; Haggett, 1976; de Wit et al., 1986). Some studies (Kella et al., 1989; Kim et al., 2005) have demonstrated that the foaming properties of β-lactoglobulin and other whey proteins are dependent on the temperature, where more extensive protein unfolding results in higher foaming capacity and foam stability. In the case of soy proteins, heat denaturation enhances its foaming properties by increasing protein surface hydrophobicity and surface activity (Carp et al., 1997).

Whipping or mixing has been employed for foam formation and can be performed using a variety of devices, e.g. kitchen mixer (Phillips et al., 1995; Camacho et al., 1998; Carp et al., 2001); turbines/impellers (Hu et al., 2003; Thakur et al., 2003); rotor–stator (Kroezen and Wassink, 1988; Hanselmann and Windhab, 1999; Muller-Fischer and Windhab, 2005) and a scraped surface heat exchanger (Djelveh et al., 1994; Djelveh and Gros, 1995). All of these methods vigorously agitate a liquid and its interface with a bulk gas phase. In the process, air is incorporated into the liquid and broken into smaller bubbles by high speed motion of an impeller which generates shear and turbulence in the mixture. In this paper, the experimental results on the foam characteristics formed by whipping air into a protein solution by mechanical action are presented. The effects of process parameters (whipper speed and geometry, solution flow rate and temperature) as well as the type of proteins on foam characteristics are discussed.

2. Materials and methods

2.1. Sample procedure

Two percent of sodium caseinate (Sigma Chemical Co., St. Louis, MO) or whey protein (Sci-Fit, Oakmont, PA) in phosphate buffer (pH 7.0 and ionic strength 0.01 M) was heated to desired temperature on a hot plate. The temperature was monitored using a thermocouple (DTR LYC, Brookfield Eng. Labs Inc., Middlebore, MA). The protein solution was continuously fed to the whipping chamber at a controlled flow rate by using a peristaltic pump (Master-Flex L/S, Coleparmer Instrument Co., Vernon Hills, IL). AC current (Fluke 189 True RMS multimeter, Fluke Corporation, Everett, WA) to the motor was recorded using a multimeter. A Data Logger (OM-320 Portable Data logger system, Omega Engineering, Inc., Stamford, CT) was used to record voltage to the motor and whipper speed. These current and voltage readings were employed to calculate the power input. The gas–liquid dispersion was collected into a plastic conical cup (5 cm bottom dia, 6 cm top dia and 8.75 cm high) for foam volume fraction measurement. The bubbles in the dispersion creamed rapidly to form a foam layer at the top and a liquid layer at the bottom. Some foam was transferred to a glass slide and imaged using a microscope. No attempt was made to measure the bubble size as a function of height. Therefore, the effect of creaming on bubble size could not be ascertained. Another sample was collected in a glass tube with the inner diameter of 13 mm and height of 20 mm for magnetic resonance imagining (MRI) analysis.

2.2. Foam volume fraction

Heights of foam and liquid were measured 2, 5 and 10 min after collecting the dispersion in the plastic cup. Since the geometry of the cup is known, the volumes of foam and liquid could be determined from their respective heights. The foam volume fraction refers to the ratio of foam volume to total volume of foam and liquid layers.

2.3. Liquid fraction in foam

The variation of liquid holdup with height was measured using MRI. Details of this technique have been described elsewhere (McCarthy, 1990; Wang and Narsimhan, 2004). The sample cell was inserted into a 20 MHz MARAN Ultra Magnetic imaging spectrometer (Resonance Instruments Ltd., Oxfordshire, UK). Sample was scanned to produce ^{1}H spectra at 15 MHz at 2, 5, 10 and 15 min after the foam was collected into a sample tube. One scan was performed for each profile which provided fairly good signal to noise ratio. The interval between 90° and 180° pulses was 3 ms, and pre-delay between successive signal acquisitions was 15 s. Typical liquid holdup profiles are shown in Fig. 2. Integration of liquid holdup over the foam height as obtained by MRI gives the liquid content in the foam; and integration of liquid holdup profile over the whole tube gives the total liquid. The liquid fraction in foam was obtained by dividing the liquid in foam by the total liquid.

2.4. Initial relative density

The relative density of gas–liquid dispersion was determined from the liquid holdup profile measured using MRI. A known volume of sample holder cup was used to fill the gas–liquid dispersion. The initial relative density is defined as

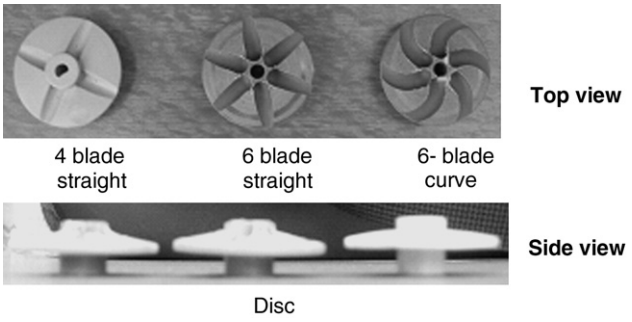

Fig. 1. Different whipper geometries.

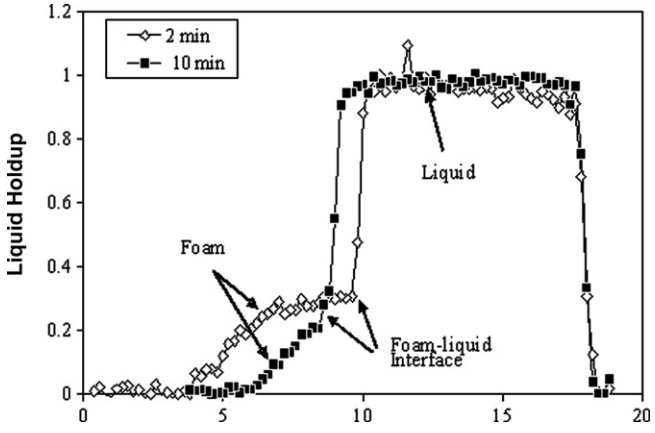

Fig. 2. Typical plots of liquid holdup at different time using MRI.

$$\rho = \frac{V_{\text{liquid}}}{V_{\text{cup}}} \tag{1}$$

where V_{liquid} is the amount of liquid in the sample holder cup, which is the integration of liquid holdup profile from MRI, and V_{cup} is the volume of sample holder cup.

2.5. Power input

The background power input of the motor was obtained by multiplying the current and voltage at desired whipper speed when operated without protein solution load. The power input under load was measured with protein solution flowing through the whipping chamber. The difference between the background and load power input is referred as net power input. The net power input divided by flow rate is the energy input per unit volume of liquid.

2.6. Apparent viscosity index

The apparent viscosities of the foams were characterized using a Brookfield viscometer (Brookfield Engineering Labs, Inc., Stoughton, MA) with a stainless steel T-spindle (Brookfield #91, 48.1 mm wide and 0.73 mm in diameter). The T-spindle was lowered to exactly the middle of the foam and the rotational speed of spindle was increased stepwise from 0.5 to 60 rotations per minute, depending on the wetness of foam. Wetter foams had lower apparent viscosity; hence the measurements could be taken up to spindle speed of 60 rpm. On the other hand, for dry foam, the measurements could only be taken up to spindle speeds of 5–10 rpm. These measurements were made at 2, 5 and 10 min after the foam was collected into a plastic cup. The rotation of the spindle in the foam was found to have insignificant effect on foam stability since the spindle was very thin. Also, in order to minimize the effect of spindle on foam stability, the rotation of the spindle was stopped soon after each viscosity measurement.

Since constant shear rate could not be maintained in a T-spindle, these measurements do not yield the "true apparent viscosity". Consequently, the "apparent viscosity" readings obtained from the instrument are a measure of torque divided by angular velocity, with a geometric factor. These readings were then converted to "apparent viscosity index" in mPa s, using,

$$\eta_{\text{app,index}} = \frac{\eta_{\text{app,foam}}}{\eta_{\text{app,glycerine}}} 1485 \tag{2}$$

where $\eta_{\text{app,foam}}$ and $\eta_{\text{app,glycerine}}$ are the apparent viscosities of foam and glycerin measured using a T-spindle in Brookfield viscometer, respectively at a certain spindle speed, the viscosity of glycerin at room temperature being 1485 mPa s (www.reference.com/browse/wiki/Viscosity).

Apparent viscosities of glycerin for different spindle speeds of 1–10 rpm were determined using a T-spindle in Brookfield viscometer. The apparent viscosity did not differ significantly as spindle speed, which is expected because

glycerin is a Newtonian fluid (data not shown). In addition, the viscosity measured was very close to the literature data (1485 mPa s).

2.7. Bubble size measurement

Small samples of foam were put in a glass slide and placed under a light microscope (Spencer) with an amplification of 80. Photographs were taken using Polaroid instant pack films. The photographs were analyzed using Scion Image Analysis software to obtain the mean bubble size as well as bubble size distribution. Around 100–300 bubbles were counted for each sample.

3. Results and discussion

Four whipper speeds (5000, 7500, 10,000 and 15,000 rpm), three whipper geometries (four-blade straight, six-blade straight and six-blade curved, see Fig. 1), four liquid flow rates (5, 7.5, 10 and 15 mL/s), two proteins (Na-caseinate and whey) and three different temperatures (21, 40 and 80 °C) were investigated. A video of the transparent mixing chamber at different liquid flow rates (not shown) indicated that more air was incorporated into the chamber at lower liquid flow rates. The volume of the whipping chamber was predominantly empty at low liquid flow rate of 5 mL/s, whereas at a higher liquid flow rate of 15 mL/s, the mixing chamber was more or less filled up.

3.1. Foamability

The initial relative density (Table 1) decreased with increasing whipper speed, because of more air incorporation and smaller bubble size, consistent with observations reported in the literature (Kroezen and Wassink, 1987; Muller-Fischer and Windhab, 2005; Djelveh et al., 1994). The initial relative density of foams also decreased at lower liquid flow rate (Table 2) since more air was incorporated as evidenced by video images of the mixing chamber (not shown here).

Na-caseinate stabilized foam formed using a six-blade disc whipper showed smaller relative density (better foamability) than whey protein stabilized foam at all temperatures (Table 3). This result is expected because casein, a random coil protein, adsorbs and spreads at the air–water interface easily, whereas whey, a globular protein, has low molecular flexibility and therefore has to overcome higher energy barrier to adsorb and spread at the interface. The interesting observation is that the foamability (relative density) of Na-caseinate decreased (increased) with increasing temperature whereas whey protein showed the opposite trend. The difference in the temperature dependence on foamability can be explained in terms of temperature dependence on molecular structure. Since Na-caseinate molecules are flexible, higher temperatures do not influence its structure. As a result, the adsorption rate and interfacial properties of the adsorbed layer are less sensitive to variations in temperature. At higher temperature, the liquid phase viscosity decreases, which can potentially have a detrimental effect on foam formation. On the other hand, the decrease in surface tension with temperature more than compensates for the detrimental effect of viscosity, resulting in an overall increase in foamability at higher temperature. Heat treatment of whey, a globular protein, increases its surface hydrophobicity because of unfolding. This increase in surface hydrophobicity reduces the energy barrier for adsorption at air–water interface, thus improving its foaming properties (Mitchell, 1986). This effect predominates over the other negative effects caused by decrease in viscosity and protein aggregation, thus resulting in an increase in foaming capacity with temperature. Some studies (deVilbiss et al., 1974; Haggett, 1976; Graham and Phillips, 1979; Kim et al., 2005) showed that partial denaturation of whey protein by heating improves foamability. However, heating above 80 °C decreased the foaming capacity.

Table 1
Effect of whipper speed on the initial relative density, power input and average bubble diameter of 2% (w/w) Na-caseinate solution formed by a six-blade-straight whipper as a function of whipper speed at 21 °C and liquid flow rate of 10 mL/s

Whipper speed (rpm)	Initial relative density	Net power input (W)	Average bubble diameter (μm)	
			Initial time	At 2 min
5000	0.77 ± 0.01	1.6 ± 0.3	66.1 ± 4.8	139.4 ± 6.1
7500	0.73 ± 0.02	4.5 ± 0.1	52.9 ± 6.7	93.7 ± 4.2
10,000	0.67 ± 0.02	7.3 ± 0.3	55.3 ± 5.1	70.3 ± 3.3
15,000	0.53 ± 0.02	16.8 ± 0.7	41.9 ± 3.4	46.7 ± 1.7

Table 2
Effect of liquid flow rate on the initial relative density, energy input and average bubble diameter of 2% (w/w) Na-caseinate solution formed by a six-blade-straight whipper as a function of liquid flow rate at 21 °C and whipper speed of 15,000 rpm

Liquid flow rate (mL/s)	Initial relative density	Energy input (J/mL)	Average bubble diameter (μm)	
			Initial time	At 2 min
5	0.48 ± 0.02	2.8 ± 0.01	51.4 ± 4.7	103.5 ± 6.5
7.5	0.51 ± 0.02	2.1 ± 0.02	50.3 ± 3.7	95.9 ± 4.7
10	0.53 ± 0.02	1.7 ± 0.07	45.2 ± 2.2	80.2 ± 4.7
15	0.63 ± 0.02	1.5 ± 0.1	47.7 ± 3.2	80.4 ± 4.9

Table 3
Initial relative density and initial average bubble size of gas–liquid dispersion of 2% (w/w) protein solution formed using a six-blade-straight disc whipper at different temperatures

Type of protein	Temperature (°C)	Initial relative density	Initial average bubble size (μm)
Na-caseinate	21	0.50 ± 0.01	45.2 ± 2.2
Na-caseinate	40	0.52 ± 0.01	50.4 ± 0.5
Na-caseinate	80	0.53 ± 0.02	52.9 ± 4.8
Whey protein	21	0.69 ± 0.01	80.2 ± 4.7
Whey protein	40	0.62 ± 0.03	89.8 ± 5.8
Whey protein	80	0.56 ± 0.02	109.3 ± 8.5

Whipper speed was 15,000 rpm and liquid flow rate was 10 mL/s.

Table 4
Effect of whipper geometry on the initial relative density, power input and average bubble diameter of 2% (w/w) Na-caseinate solution formed by different whippers at 80 °C

Type of whipper	Initial relative density	Net power input (W)	Average bubble diameter (μm)	
			Initial time	At 2 min
Four-straight	0.57 ± 0.02	10.8 ± 0.30	66.1 ± 4.8	115.1 ± 12.7
Six-straight	0.53 ± 0.02	13.1 ± 0.29	52.9 ± 6.7	109.3 ± 8.5
Six-curve opposite	0.52 ± 0.01	14.0 ± 0.10	55.3 ± 5.1	114.4 ± 5.4
Six-curve parallel	0.58 ± 0.02	12.9 ± 0.31	41.9 ± 3.4	96.7 ± 6.7

Whipper speed was 15,000 rpm and liquid flow rate was 10 mL/s.

An increase in foamability was observed when increasing the number of blades from 4 to 6 (Table 4, Fig. 3d), consistent with the observations (Kroezen and Wassink, 1987; Kroezen and Wassink, 1988) that mixing capacity increased linearly with the number of rotor–stator units. Djelveh et al. (1994) also observed that increasing the number of paddles/blades in a scrapped surface heat exchanger resulted in lower product density. Furthermore, to study the effect of whipper geometry on six-blade whipper, a six-blade with curve configuration was made. A unique feature of this whipper is that it can be operated in two directions: opposite and parallel to the curvature of vanes. Interestingly, different directions showed significantly different foamability. When the whipper is rotated in the direction opposite to the curvature of vanes, it behaved like a centrifugal pump and drew more air into the whipping chamber, which resulted in higher foam volume compared to that formed when the whipper was operated parallel to the curvature.

3.2. Foam stability

Foam volume fraction increased as whipper speed increased due to more air incorporation; and the liquid fraction was also found to be higher as a result of more entrainment of liquid in the foam resulting from smaller bubble size as shown in Table 1 and Fig. 3a. The plot of foam volume fraction and liquid fraction in foam for different liquid flow rates is shown in Fig. 3b. Because of greater air incorporation at lower liquid flow rate, a higher foam volume fraction was observed (Fig. 3b, Table 2). The foam was also wetter because of higher liquid entrainment (Fig. 3b). The liquid fraction in foam showed the same trend as the initial relative density (Table 2) and foam volume fraction (Fig. 3b).

Both, the foam volume fraction and liquid fraction in foam were higher for the foams formed in Na-caseinate than in whey protein at short times (Fig. 3c) indicating that foamability of Na-caseinate is higher than whey protein, consistent with earlier observations (Graham and Phillips, 1979; Dickinson and Stainsby, 1982). However, both the foam volume fraction as well as liquid in foam decreased much faster for foams stabilized by Na-caseinate. While this decrease in liquid fraction in foam was due to liquid

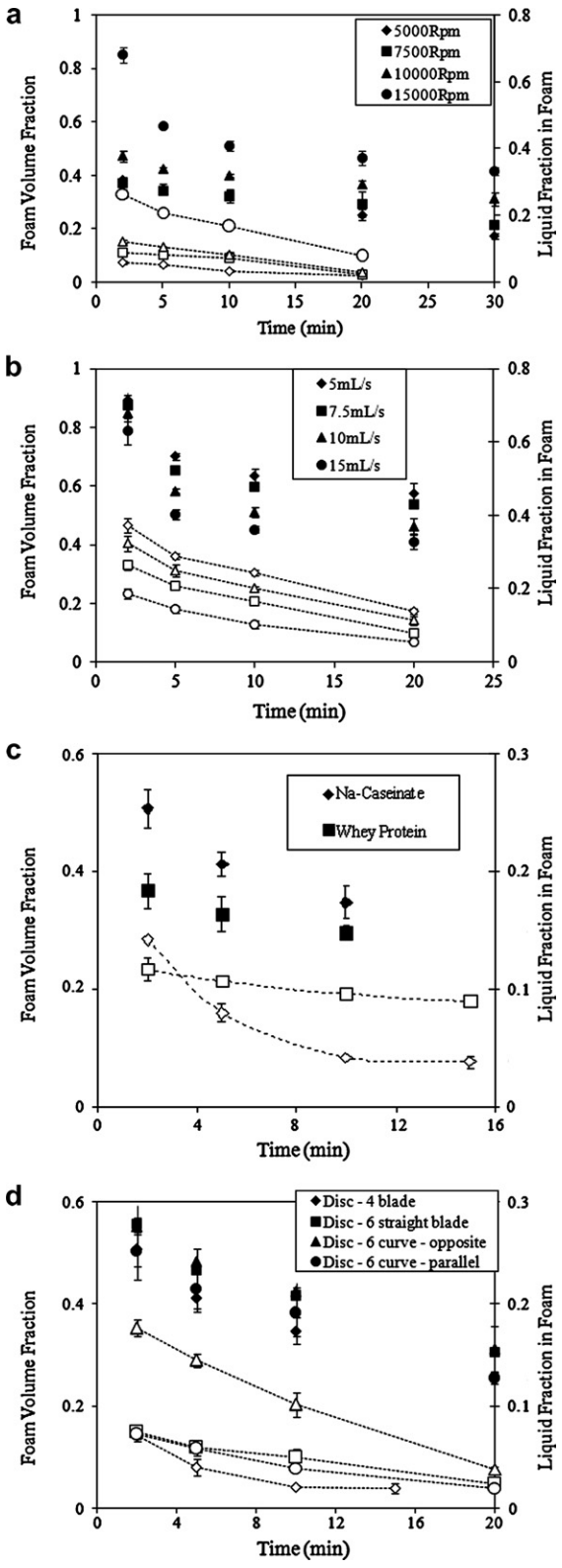

Fig. 3. Foam volume fraction (closed symbols) and liquid fraction in foam (open symbols) as a function of time for: (a) different whipper speeds; the experimental conditions were same as given in Table 1. (b) Different liquid flow rates; the experimental conditions were same as those given in Table 2. (c) Two different proteins; the temperature is 80 °C and other experimental conditions are the same as those given in Table 3. (d) Different whippers; the experimental conditions are same as those stated in Table 4.

drainage, the decrease in foam volume was due to the combined effects of syneresis as well as bubble coalescence. These results suggest that Na-caseinate stabilized foams are less stable than those stabilized by whey protein (Phillips, 1981). At longer times, the foam volume fractions for Na-caseinate stabilized foams were found to be higher than those stabilized by whey protein, whereas the liquid fraction in foams stabilized by whey protein was higher than those stabilized by Na-caseinate. Such a difference indicates that the foam formed with whey protein is much wetter than that formed with Na-caseinate at longer times. This was also confirmed by MRI profile (data not shown). As a flexible protein, Na-caseinate imparts lower surface viscosity and surface elasticity to the adsorbed layer at air–water interface than whey protein. Higher surface viscosity and elasticity imply lower surface mobility, which reduces liquid drainage and resists thin film rupture (Narsimhan and Wang, 2005; Wang and Narsimhan, 2005). Smaller film rupture rate would result in smaller bubble size, which in turn reduces the liquid drainage rate (Narsimhan and Wang, 2005). Although other factors such as surface tension, charge, molecular configuration may also affect the liquid drainage and film stability due to the change of disjoining pressure profile and equilibrium film thickness (Wang and Narsimhan, 2005), the effects of surface rheology may play a dominant role here.

Both the foam volume fraction and liquid fraction in foam were higher at lower temperature, whilst decreasing with time (Fig. 4a). A larger decrease in foam volume fraction was observed at 80 °C whereas this decrease was more pronounced for liquid fraction in foam as the temperature was increased from 21 to 40 °C. At higher temperatures, the liquid viscosity was lower and bubble size was larger, which tended to increase liquid drainage (Mita et al., 1977; Halling, 1981; Narsimhan and Wang, 2005). In addition, lower surface tension at higher temperature also had a destabilizing influence, thus increasing bubble size and therefore liquid drainage. On the other hand, the foam was wetter at lower temperature and the liquid drainage rate was faster. The net effect is better foam stability at lower temperature for Na-caseinate stabilized foams. Patino et al. (1995) observed that casein stabilized foams were more stable at room temperature. The stability was independent of temperature between 5 and 20 °C, although it reduced significantly above 20 °C.

Foams produced at room temperature were highly unstable and almost all foams disappeared after 10 min (Fig. 4b). The rate of decrease in foam volume slowed down considerably at higher temperatures with insignificant difference in the rates being observed between 40 and 80 °C (Fig. 4b). However, more foam was produced at 80 °C compared to 40 °C (Fig. 4b). More liquid was entrained in foams that were produced at higher temperatures though the subsequent rates of liquid drainage were found to be temperature independent (Fig. 4b). Therefore, the foam stability increased with temperature. It has been shown (Kim et al., 2005) that partial denaturation due to heating results in an increase in the surface hydrophobicity of β-lactoglobulin which, in turn, leads to higher surface activity and an improvement in surface rheological properties at air–water and oil–water interfaces. Kim et al. (2005) showed that the there is one to one correspondence between surface rheological properties and emulsion/foam stability of heat treated β-lactoglobulin.

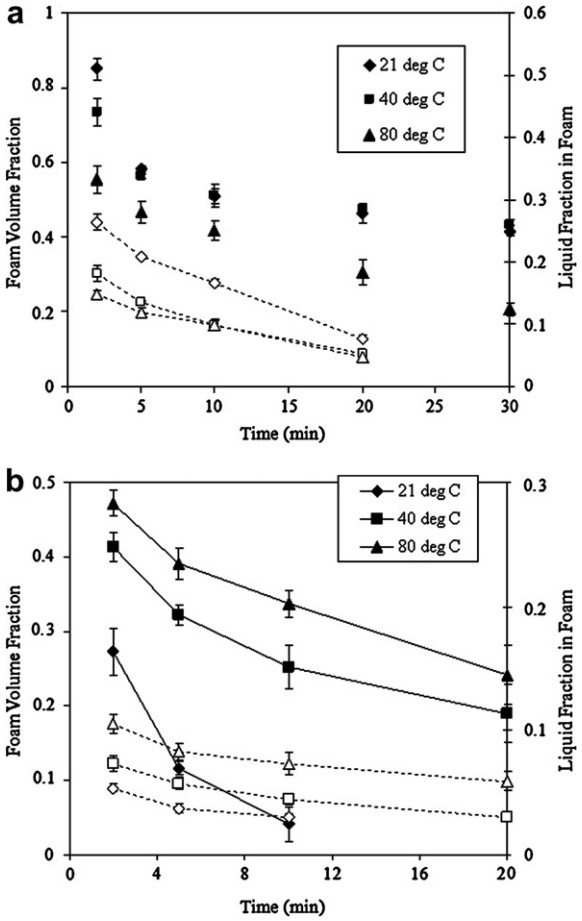

Fig. 4. The foam volume fraction (closed symbols) and liquid fraction in foam (open symbols) of gas–liquid dispersion as a function of time (a) foam formed with 2% (w/w) Na-caseinate solution at different temperatures; the experimental conditions are given in Table 3. (b) Foam formed with 2% (w/w) whey protein solution formed at different temperatures; the experimental conditions are given in Table 3.

For all whipper geometries, the foam volume fraction decreased with time due to the collapse of foam bubbles at the top (Fig. 3d). The liquid fraction in foam also decreased with time due to foam drainage. Foams formed by all six-blade whippers showed higher foam volume fraction and liquid fraction in foam than four-blade whipper, suggesting that increasing the number of blades results in better foam behavior (Fig. 3d). The six-curve-blade whipper operated in opposite direction produced foam with highest foam volume fraction and liquid fraction.

3.3. Power input

Because of more air incorporation at higher whipper speed, a higher power input was required (Table 1), this

is consistent with observations reported in the literatures (Kroezen and Wassink, 1987; Windhab, 1991; Hanselmann and Windhab, 1999; Muller-Fischer and Windhab, 2005). As expected, the net power input for foam formation was higher at higher liquid flow rate (data not shown). However, the power input per unit volume of liquid was higher at lower liquid flow rate (Table 2) because of greater levels of air incorporation which requires creation of more gas–liquid interfacial area. However, the evaluation of interfacial energy per unit volume of the liquid based on the bubble size and interfacial tension indicated that this surface energy is very small (of the order of mJ/mL) thus suggesting that most of the energy input was expended as viscous dissipation.

Among different whippers, four-blade disc whipper, which produced the least foam, required the lowest power input (Table 4). Six-blade-curve disc whipper running opposite to the curvature, produced the most foam and therefore, required highest power input (Table 4), consistent with observation by other researchers that higher power input was required as the number of rotor–stator pairs was increased (Muller-Fischer and Windhab, 2005) and number of paddles was increased (Djelveh and Gros, 1995).

3.4. Apparent viscosity index

The apparent viscosity index of foams produced at four different whipper speeds were measured at different spindle speeds of the rheometer. These measurements were made 2, 5 and 10 min after dispensation of the gas–liquid dispersions and are shown in Figs. 5a–c, respectively. Results indicate that the foams are shear thinning in that the apparent viscosity index decreases with rpm of the spindle. As shown in Figs. 5a and b, the apparent viscosity index of foams formed at higher whipper speeds was lower. The smaller value of apparent viscosity index indicates that the foam is wetter. Also, the foam formed at lower spindle speed is found to be more shear thinning. The foam formed at the highest spindle speed of 15,000 rpm exhibited a much lower apparent viscosity index than those formed at lower speeds. This trend is in good agreement with results reported above which indicate that, higher whipper speed produce more foam (Table 1 and Fig. 3a), with higher liquid fraction (Fig. 3a). For dispersions having relatively large liquid fractions, the apparent viscosity decreases with an increase in air volume fraction. In foams, the air bubbles are distorted in the form of a polyhedral structure. The liquid in the foam is distributed between thin films and Plateau borders. As time progresses, liquid in thin films drains into neighboring Plateau borders because of Plateau border suction resulting from the radius of curvature of Plateau border. In addition, the liquid drains due to gravity through the network of Plateau borders leading to accumulation of liquid layer at the bottom. As a result, the foam becomes drier at the top and wetter at the bottom and the amount of liquid that is accumulated increases. This results in a gradient in Plateau border suction that opposes gravity. Consequently, at suffi-

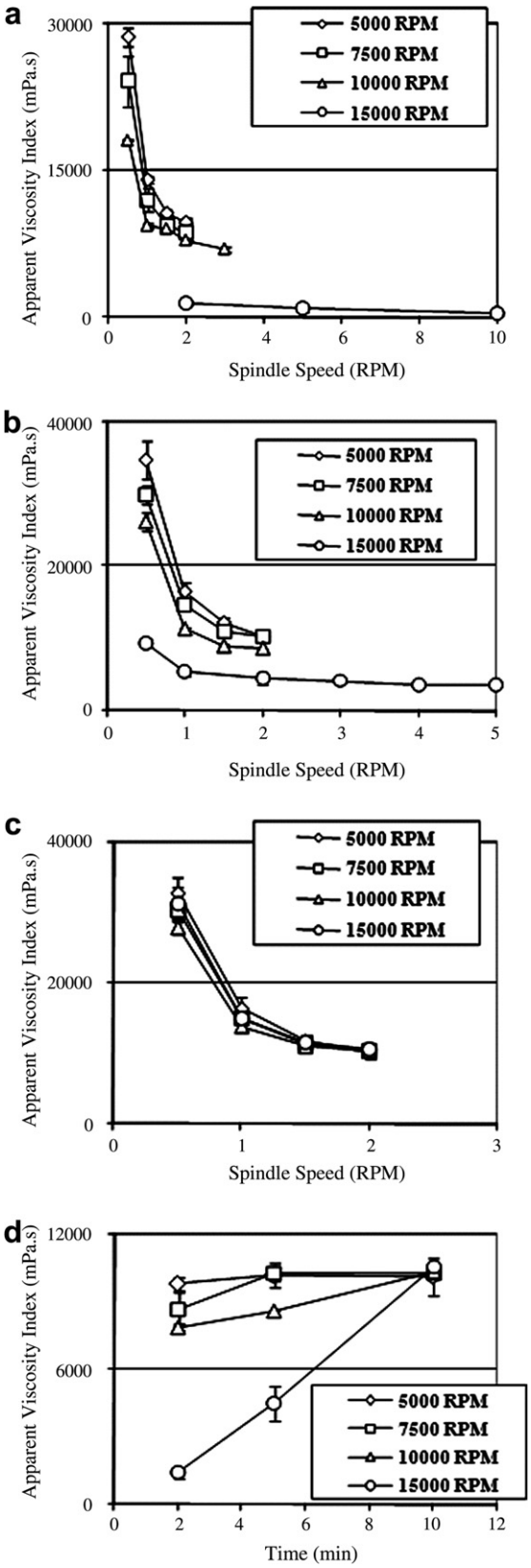

Fig. 5. The apparent viscosity index as a function of spindle speed at different times after dispensation of the foams formed at different whipper speeds. (a) 2 min after dispensation, (b) 5 min after dispensation, (c) 10 min after dispensation and (d) apparent viscosity index as a function of time at a constant spindle speed of 2 rpm. Experimental conditions are given in Table 1.

ciently long times, no further liquid drainage occurs and the foam reaches a mechanical equilibrium at which the gravity is counterbalanced by the gradient of Plateau border suction. Drier foams exhibit higher apparent viscosity (Prodhomme and Khan, 1996). Therefore, there is an increase in the apparent viscosity of foam with time for all whipper speeds as shown by apparent viscosity index values in Fig. 5d. Since the foam that was formed at the highest whipper speed of 15,000 rpm was the wettest, it exhibited the most rapid drainage. This is reflected in the most significant increase in the apparent viscosity index of the foam (Fig. 5d). Also, the apparent viscosity versus spindle speed (shear rate) profile of foams produced at different whipper speeds coincide at 10 min after dispensation (Fig. 5c), thus indicating that the liquid holdup in these foams approaches a mechanical equilibrium as explained above. In addition, at longer times, as the foam becomes drier, the bubbles coalesce because of rupture of thin films separating them thus leading to an increase in average bubble size with time as shown in Table 1.

The apparent viscosity index was lower at lower inlet liquid flow rates since the foam was wetter (Table 5 and Fig. 3b). The apparent viscosity index of foams increased with time since the foams became drier as a result of liquid drainage (Table 5, Figs. 3a,b and 5). The apparent viscosity of foam is also affected by the bubble size. Experimental measurements of apparent viscosity of concentrated emulsion as model foam systems showed an increase in apparent viscosity for smaller particle (droplet) size (Prodhomme and Khan, 1996). Bubble size was smaller for foams formed at higher liquid flow rates (Table 2) thus contributing to higher apparent viscosity. However, at higher rpm, the effect of smaller bubble size (Table 1) is compensated by higher liquid fraction (Fig. 3a) thus resulting in smaller apparent viscosity.

Foams formed using sodium caseinate had a lower apparent viscosity index than those formed using whey protein (Table 5). The low apparent viscosity index indicates wetter foam, where more liquid is entrapped in the foam. This trend is in good agreement with other experimental results, as shown in Fig. 3c (the foamability and amount of liquid entrapped of these proteins followed the order of sodium caseinate > whey protein). As expected, the apparent viscosity index increased from 2 to 5 min due to liquid drainage. However, the apparent viscosity index later decreased from 5 to 10 min after dispensation for Na-caseinate stabilized foams. This decrease could be explained by the increase in bubble size as a result of coalescence. As bubble size increases, the torque required to rotate the spindle is lower, thus resulting in a decrease of apparent viscosity index. However, for whey protein stabilized foams, the effect of coarsening of bubbles due to coalescence dominated over the drainage effect, which resulted in a constant decrease of apparent viscosity index from 2 to 10 min, as shown in Table 5.

Lower apparent viscosity index was observed at lower temperature for sodium caseinate stabilized foam as a result of it being wetter (Table 5, Fig. 4a). The apparent viscosity indices of foams increased from 2 to 10 min for all temperatures as a result of liquid drainage. For whey protein stabilized foam, the apparent viscosity followed the same trend as the observations for the foams stabilized by sodium caseinate. Foams produced at higher temperatures were drier.

The experimental results show that six-blade-curve disc whipper operated in the direction opposite to the curvature of vanes produced most foam (Fig. 3d), hence, entrapped most liquid as compared to the other whipper geometries. As a result, the foams produced were wetter, with lower apparent viscosity indices (Table 5). The apparent viscosity index increased from 2 to 5 min as a result of liquid drainage. However, this parameter decreased from 5 to 10 min after dispensation due to the coarsening of bubble size.

Table 5
The apparent viscosity index of foams formed at different conditions at a spindle speed of 2 rpm

Effect		Apparent viscosity index (mPa s)		
		2 min	5 min	10 min
Whipper speed[a] (rpm)				
5000		14,137 ± 290	10,197 ± 532	10,131 ± 873
7500		8707 ± 726	10,250 ± 296	10,263 ± 262
10,000		7900 ± 125	8631 ± 332	10,356 ± 165
15,000		1702 ± 250	4498 ± 395	10,604 ± 658
		2 min[e]	5 min	10 min
Liquid flow rate[b] (mL/s)				
5		~100	3530 ± 76	10,728 ± 150
7.5		~100	4497 ± 595	9457 ± 350
10		~100	4998 ± 695	10,004 ± 258
15		~100	5374 ± 495	9619 ± 178
Type of protein[c]	Temperature (°C)	2 min	5 min	10 min
Na-caseinate	21	1702 ± 250	4498 ± 395	10,604 ± 658
Na-caseinate	40	3832 ± 248	7798 ± 308	11,237 ± 961
Na-caseinate	80	5670 ± 146	8165 ± 667	6487 ± 589
Whey protein	21	925 ± 94	[f]	[f]
Whey protein	40	3631 ± 391	7135 ± 442	6109 ± 632
Whey protein	80	10,136 ± 748	9285 ± 567	8754 ± 574
Whipper geometry[d]				
Four-blade		5172 ± 201	5516 ± 424	4307 ± 185
Six-blade-straight		5670 ± 146	8165 ± 467	7990 ± 280
Six-blade-curve-opposite		3636 ± 521	6065 ± 138	5424 ± 485
Six-blade-curve-parallel		6975 ± 480	7217 ± 142	7004 ± 348

[a] Conditions are the same as those given in Table 1.
[b] Conditions are the same as those given in Table 2.
[c] Conditions are the same as those given in Table 3.
[d] Conditions are the same as those given in Table 4.
[e] The foams were very wet, the Brookfield gave very low apparent viscosity.
[f] All foams were ruptured in 5 min.

3.5. Bubble size

As expected, the bubble size decreased as whipper speed increased (Table 1) consistent with observations by other researchers (Kroezen and Wassink, 1987; Windhab, 1991;

Muller-Fischer and Windhab, 2005). The average bubble size of the dispersion immediately after formation and 2 min thereafter, for different liquid flow rates, are shown in Table 2. Immediately after foam formation, the average bubble size decreased as the inlet liquid flow rate increased, this decrease being more pronounced at lower whipper speeds (data not shown). As expected, an increase in the mean bubble size with time was observed for all inlet liquid flow rates, due to bubble coalescence. Higher coalescence rate was observed at lower inlet liquid flow rate. This can be attributed to more air incorporation, which resulted in higher rate of collision of bubbles, and hence, higher rate of coalescence.

The average initial bubble size of foams formed using Na-caseinate and whey protein solutions increased with temperature (Table 3). Increase in temperature increases thermal motion, which results in a higher coalescence rate. Since Na-caseinate is more surface active than whey protein, it can adsorb faster at the air–water interface during foam formation. In addition, because of its flexibility, Na-caseinate can rearrange itself at the interface much faster, thus decreasing the surface tension. Consequently, it is easier to breakup the bubbles during foam formation using Na-caseinate than whey. As a result, the bubble sizes were found to be smaller for the former (see Table 3). The effect of temperature on bubble size was more pronounced for foams formed using whey.

An increase in bubble size with time was observed for foams formed with sodium caseinate for all whipper geometries (Table 4). Increasing the number of blades of disc whipper reduced the bubble size by approximately 20%, and operating the curved whipper in the direction parallel to the curvature of the vanes produced the smallest bubbles. This trend has also been observed by other researchers (Djelveh and Gros, 1995; Muller-Fischer and Windhab, 2005).

4. Conclusion

Foam was formed by continuous whipping of 2% protein (Na-caseinate and whey protein) solutions. The effects of whipper geometry, whipping speed, liquid flow rate and temperature on the foaming properties such as foamability, foam stability, energy input and bubble size were investigated. Increasing the number of blades in whipper from 4 to 6 improved the foaming efficiency. Among whippers with 6 blades, the whipper with curved blades operating in the direction opposite to the curvature of the vanes showed highest foamability, while operating in a direction parallel to the curvature produced the smallest bubbles. High whipping speed and lower liquid flow rate were favorable for foam formation and stability. The energy input to liquid depended on the amount of air incorporated into the dispersion. Na-caseinate, due to its flexible molecules, showed much better foamability but poorer foam stability than whey protein. Increase in temperature improved the foamability and foam stability for foams formed using whey protein, whereas Na-caseinate showed the opposite trend. Whey protein produced larger bubble size than Na-caseinate, this difference being more significant at higher temperature.

Acknowledgement

We would like to acknowledge Nestle R&D center, New Milford CT for providing the financial support to carry out the work reported here.

References

Buckingham, J.H., 1970. Effect of pH, concentration and temperature on the strength of cytoplasmic protein foams. Journal of the Science of Food and Agriculture 21, 441–445.

Camacho, M.M., Martinez-Navarrete, N., et al., 1998. Influence of locust bean gum/gamma-Carrageenan mixture of whipping and mechanical properties and stability of dairy creams. Food Research International 31, 653–658.

Carp, D.J., Wagner, J., et al., 1997. Rheological method for kinetics of soy proteins foams. Journal of Food Science 62 (6), 1105–1109.

Carp, D.J., Bartholomai, G.B., et al., 2001. Effect of denaturation on soy-protein–Xanthan interactions: comparison of a whipping-rheological and bubbling method. Colloids and Surfaces B: Biointerfaces 21, 163–171.

Cho, D., Narsimhan, G., et al., 1996. Adsorption dynamics of native and alkylated derivatives of bovine serum albumin at air–water interface. Journal of Colloid and Interface Science 178 (1), 348–357.

Cho, D., Narsimhan, G., et al., 1997. Adsorption dynamics of native and pentylated bovine serum albumin at air–water interface: surface concentration/surface pressure measurements. Journal of Colloid and Interface Science 191 (2), 312–325.

Cornec, M., Kim, D.A., Narsimhan, G., 2001. Adsorption dynamics and interfacial properties of alpha-lactalbumin in native and molten globule state conformation at air–water interface. Food Hydrocolloids 15 (3), 303–313.

Damodaran, S., 1996. Functional properties. In: Nakai, S., Modler, H.W. (Eds.), Food Proteins – Properties and Characterization. VCH Publisher, New York, pp. 167–234.

deVilbiss, E.D., Holsinger, V.H., et al., 1974. Properties of whey protein concentrate foams. Food Technology 28 (3), 40–48.

de Wit, J.N., Klarenbeek, G., et al., 1986. Evaluation of functional properties of whey protein concentrates and whey protein isolates: 2. Effects of processing history and composition. Netherlands Milk Dairy Journal 40, 41–56.

Dickinson, E., Stainsby, G., 1982. Colloids in Foods. Applied Science Publishers Ltd., New York.

Djelveh, G., Gros, J.B., 1995. Estimation of physical properties of foamed foods using energy dissipation in scraped-surface heat exchangers. Journal of Food Engineering 26 (1), 45–56.

Djelveh, G., Bacati, O., et al., 1994. Mechanical aspects of gas dispersion in continuous foaming food processes using scraped surface heat exchangers. Journal of Food Engineering 23 (2), 213–223.

Graham, D.E., Phillips, M.C., 1976. The conformation of proteins at the air–water interface and their role in stabilizing foams. In: Akers, R.J. (Ed.), Foams. Academic Press, London, pp. 237–255.

Graham, D.E., Phillips, M.C., 1979. Proteins at liquid interfaces: I. Kinetics of adsorption and surface denaturation. Journal of Colloid and Interface Science 70 (3), 403–414.

Graham, D.E., Phillips, M.C., 1980. Proteins at liquid interfaces: IV. Dilatational properties. Journal of Colloid and Interface Science 76 (1), 227–239.

Haggett, T.O.R., 1976. The whipping, foaming and gelling properties of whey protein concentrates. New Zealand Journal of Dairy Science and Technology 11, 244–250.

Halling, P.J., 1981. Protein stabilized foams and emulsions. CRC Critical Review in Food Science Nutrition 15, 155–203.

Hanselmann, W., Windhab, E., 1999. Flow characteristics and modelling of foam generation in a continuous rotor/stator mixer. Journal of Food Engineering 38, 393–405.

Hu, B., Nienow, A.V., et al., 2003. The effect of sodium caseinate concentration and processing conditions on bubble sizes and their break-up and coalescence in turbulent batch air/aqueous dispersions at atmospheric and elevated pressures. Colloids and Surfaces B: Biointerfaces 31, 3–11.

Kella, N.K., Yang, T., et al., 1989. Effects of disulfied bond cleavage on structural and interfacial properties of whey proteins. Journal of Agricultural and Food Chemistry 37, 1203–1210.

Kim, D., Cornec, M., et al., 2005. Effect of thermal treatment on interfacial properties of beta-lactoglobulin. Journal of Colloid and Interface Science 285 (1), 100–109.

Kroezen, A.B.J., Wassink, G.J., 1987. Bubble size distribution and energy dissipation in foam mixers. JSDC 103, 387–394.

Kroezen, A.B.J., Wassink, G.J., 1988. Foam generation in a rotor–stator mixer. Chemical Engineering and Processing 24 (3), 145–146.

Martin, A.H., Grolle, K., et al., 2002. Network forming properties of various proteins adsorbed at air/water interface in relation to foam stability. Journal of Colloid and Interface Science 254, 175–183.

McCarthy, M.J., 1990. Interpretation of the magnetic resonance imaging signal from a foam. AICHE Journal 36 (2), 287–290.

Mita, T., Ishido, E., et al., 1977. Physical studies on wheat protein foams. Journal of Colloid and Interface Science 59, 172–178.

Mita, T., Ishido, E., et al., 1978. Physicochemical studies on wheat protein foams: II. Relationship between bubble size and stability of foams prepared with gluten and gluten components. Journal of Colloid and Interface Science 64 (1), 143–153.

Mitchell, J.R., 1986. Development in Food Proteins. Elsevier Applied Science Publishers, New York.

Muller-Fischer, N., Windhab, E.J., 2005. Influence of process parameters on microstructure of food foam whipped in a rotor–stator device within a wide static pressure range. Colloids and Surfaces A: Physicochemical and Engineering Aspects 263, 353–362.

Narsimhan, G., Uraizee, F., 1992. Kinetics of adsorption of globular proteins at an air–water interface. Biotechnology Progress 8 (3), 187–196.

Narsimhan, G., Wang, Z., 2005. Stability of thin stagnant film on a solid surface with a viscoelastic air–liquid interface. Journal of Colloid and Interface Science 291 (1), 296–302.

Oortwijn, H., Walstra, P., 1979. The membranes of recombined fat globules. 2. Composition. Netherlands Milk Dairy Journal 33, 134–154.

Patino, J.M.R., Delgado, M.D.N., et al., 1995. Stability and mechanical strength of aqueous foam containing food proteins. Colloids and Surfaces A: Physicochemical and Engineering Aspects 99 (1), 65–78.

Phillips, M.C., 1981. Protein conformation at liquid interfaces and its role in stabilizing emulsions and foams. Food Technology 35, 50–57.

Phillips, L.G., Hawks, S.E., et al., 1995. Structural characteristics and foaming properties of beta-lactoglobulin: effects of shear rate and temperature. Journal of Agricultural and Food Chemistry 43, 613–619.

Prins, A., 1988. Principles of foam stability. In: Dickinson, E., Stainsby, G. (Eds.), Advances in Food Emulsions and Foams. Elsevier Applied Science, London, pp. 91–123.

Prodhomme, R.K., Khan, S.A., 1996. Foams: theory, measurements and applications. In: Prodhomme, R.K., Khan, S.A. (Eds.), . In: Surfactant Science Series, vol. 57. Marcel-Dekker Inc., New York, pp. 217–240.

Thakur, R.K., Vial, C.H., et al., 2003. Influence of operating conditions and impeller design on the continuous manufacturing of food foams. Journal of Food Engineering 60, 9–20.

Wang, Z., Narsimhan, G., 2004. Evolution of liquid holdup profile in a standing protein stabilized foam. Journal of Colloid and Interface Science 280 (1), 224–233.

Wang, Z., Narsimhan, G., 2005. Interfacial dilatational elasticity and viscosity of ß-lactoglobulin at air–water interface using pulsating bubble tensiometry. Langmuir 21 (10), 4482–4489.

Windhab, E.J., 1991. Zur Technologie geschaumter Stoffsysteme im Lebens-mittelbereich, Teil 2. Lebensmitteltechnik 4, 181–183.

Yu, M.A., Damodaran, S., 1991. Kinetics of protein foam destabilization: Evaluation of a method using bovine serum albumin. Journal of Agricultural and Food Chemistry 39, 1555–1562.